

LETTERS

The Structure of a Rh/TiO₂ Catalyst in the Strong Metal-Support Interaction State As Determined by EXAFS

D. C. Koningsberger,* J. H. A. Martens, R. Prins,

Laboratory for Inorganic Chemistry and Catalysis, Eindhoven University of Technology, 5600 MB Eindhoven, The Netherlands

D. R. Short,†

Center for Catalytic Science and Technology, Department of Chemical Engineering, University of Delaware, Newark, Delaware 97111

and D. E. Sayers

Department of Physics, North Carolina State University, Raleigh, North Carolina 27695
(Received: February 7, 1986)

Reduction of a highly dispersed 2.85 wt % Rh/TiO₂ catalyst at 473 K after previous calcination at 623 K resulted in EXAFS whose primary contributions are due to nearest rhodium (average coordination number of 3.1 and distance of 2.67 Å) and oxygen neighbors (coordination 2.5 and distance 2.71 Å). These oxygen neighbors originated at the metal-support interface. The average rhodium-rhodium coordination number did not change in the SMSI state produced by reducing the catalyst at 673 K. However, the average coordination distance contracted by 0.04 Å with an accompanying decrease of the Debye-Waller factor of the Rh-Rh bond of 0.0012 Å². This is due to the fact that in the SMSI state the surface of the metal particles is not covered with chemisorbed hydrogen. The SMSI state leads to a structural reorganization of the support in the vicinity of the rhodium metal particles. This can be concluded from the appearance of a Rh-Ti bond at 3.42 Å in the SMSI state coupled with the fact that the average coordination number of the rhodium-support oxygen bonds does not increase. Other types of rhodium-oxygen bonds could not be detected with EXAFS in this state. Thus, these results provide no evidence for coverage of the metal particle by a suboxide of TiO₂ in the SMSI state.

Introduction

High-temperature reduction drastically diminishes the capacity of TiO₂-supported metal particles to adsorb H₂ or CO. Since this suppression was first accredited to an interaction between the metal

and the support, it was called the strong metal-support interaction (SMSI). Several models have been proposed to explain SMSI, such as alloy formation,¹ the electronic influence of a suboxide of TiO₂ beneath the metal particles,² and covering of the metal

† Current address: Engineering Technology Laboratory, Experimental Station, E.I. Dupont de Nemours and Co., Wilmington, DE 19898.

(1) Tauster, S. J.; Fung, S. C. *J. Am. Chem. Soc.* **1978**, *100*, 415.
(2) Horsley, J. A. *J. Am. Chem. Soc.* **1979**, *101*, 2870.

TABLE I: Fourier Transform Ranges of Reference Compounds and Crystallographic Data

| ref compd | k^n | $\Delta k^n, \text{\AA}^{-1}$ | $\Delta R, \text{\AA}$ | $R_{\text{ref}}, \text{\AA}$ | N_{ref} | ref |
|--------------------------------|-------|-------------------------------|------------------------|------------------------------|------------------|-----|
| Rh foil | k^3 | 2.68–24.4 | 1.5–3.05 | 2.687 | 12 | 11 |
| Rh ₂ O ₃ | k^1 | 2.7–18 | 0–2.05 | 2.05 | 6 | 12 |
| RhTi alloy ^a | k^1 | 2.79–12.5 | 0–3.12 | 2.676 | 8 | 13 |

^aFourier transformation after subtraction of a calculated Rh–Rh EXAFS ($N = 4, R = 2.949 \text{\AA}, \Delta\sigma^2 = 0.006 \text{\AA}^2$) from experimental data.

particles by a suboxide of TiO₂ after a reduction at high temperature.³

Extended X-ray absorption fine structure (EXAFS) is an excellent tool to investigate local structure around a metal atom in a catalyst.⁴ Recently, the existence of 2.7- \AA Rh–O (Rh⁰–O²⁻ support) bonds in the metal–support interface in highly dispersed Rh/Al₂O₃ catalysts has been reported.^{5,6} Similar Rh–O bonds were found in a Rh/TiO₂ catalyst reduced at 473 K.⁷

Here we present an EXAFS study of a 2.85 wt % Rh/TiO₂ catalyst after low (non-SMSI) and high temperature (SMSI state) reduction in order to make a careful study of the structural changes between the two states. The catalyst was very highly dispersed, which is vital for this type of study since only metal atoms in the interface will be sensitive to effects due to the support and only metal atoms on the surface will be sensitive to effects due to coverage.

Experimental Section

A 2.85 wt % Rh/TiO₂ catalyst was prepared by ion exchange using Rh(NO₃)₃ and anatase (130 m² g⁻¹, 0.63 mL g⁻¹). After adsorption, the catalyst was dried overnight at 383 K, subsequently calcined for 2 h at 623 K, and stored for further use. The dried and calcined catalyst was pressed into a thin self-supporting wafer and mounted in an in situ EXAFS cell.⁸ The thickness of the wafer was chosen to give $\mu x \approx 2.5$ at the rhodium K-edge. The reduction was carried out under flowing H₂ for 2 h at 473 K with the temperature being increased at a rate of 2.5 K min⁻¹. The sample was then cooled to room temperature under flowing H₂, and EXAFS spectra were recorded at 90 K with the catalyst exposed to 1 atm of static hydrogen. The same procedure was applied for the subsequent reduction at 673 K.

The EXAFS spectra of the rhodium K-edge were recorded in situ on X-ray beam line I-5 at the Stanford Synchrotron Radiation Laboratory (SSRL) with a ring energy of 3 GeV and ring currents between 40 and 80 mA.

Data Analysis and Results

The high-quality raw EXAFS spectra for the sample reduced at 473 and 673 K are shown in Figure 1, a and d, respectively. The data were obtained from the X-ray absorption spectrum by a cubic spline background subtraction.⁹ Normalization was performed by division to the height of the edge.⁵ Reference compounds which were used to obtain phase and backscattering functions were analyzed in the same way^{5,10} as the catalyst samples.

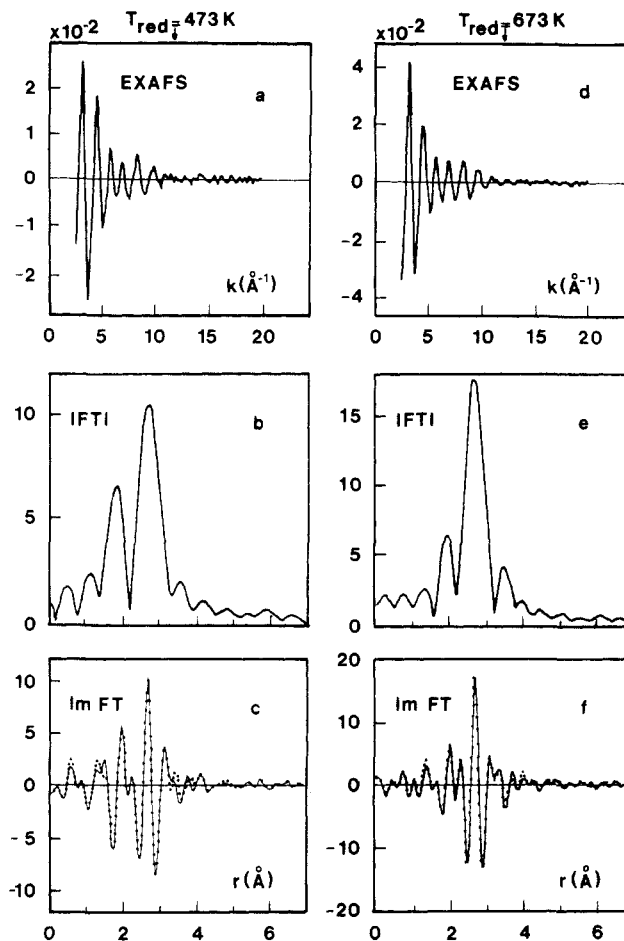


Figure 1. (a, d) Rh K-edge EXAFS data for the normal (473 K reduction) (a) and SMSI state (673 K reduction) (d) of the 2.85 wt % Rh/TiO₂ catalyst. (b, e) Magnitude of the Fourier transform of the EXAFS data of the normal (b) and SMSI state (e). The transforms were taken by using k^3 weight over a range of 4–10 \AA^{-1} and are corrected for the Rh–Rh phase and amplitude. (c, f) Comparison of the imaginary parts of the Fourier transform of the experimental (solid lines) and calculated (dashed lines) data. (c) The normal state is compared with a calculated Rh–Rh + Rh–O spectrum. (f) The SMSI state is compared with a calculated Rh–Rh + Rh–O + Rh–Ti spectrum.

Table I gives the crystallographic data and Fourier transform ranges of the reference compounds.

The magnitudes of the k^3 -weighted Fourier transforms of the experimental data obtained after reduction at 473 and 673 K are displayed in Figure 1, b and e, respectively. Before Fourier transformation the raw experimental data were smoothed by removing noise (harmonic numbers higher than 200) via Fourier filtering.⁵ The Fourier transforms are corrected for the Rh–Rh phase shift and backscattering amplitude. Reliable data for phase and backscattering amplitude have been obtained from EXAFS measurements on rhodium foil.⁵ If only a single rhodium coordination shell was present, the Rh–Rh phase and amplitude corrected Fourier transform should have shown one single symmetrical peak whose maximum was at the proper Rh–Rh distance. Clearly, in both EXAFS spectra there are other contributions present. To separate these contributions from the dominant Rh–Rh contribution and to determine their structural parameters, the difference file technique and the use of phase and/or amplitude corrected Fourier transforms have been applied. These data analysis procedures have been extensively described in ref 5 and

(3) Meriaudeau, P.; Dutel, J. F.; Dufaux, M.; Naccache, C. *Stud. Surf. Sci. Catal.* **1982**, *11*, 95. Santos, J.; Phillips, J.; Dumesic, J. A. *J. Catal.* **1983**, *81*, 147. Cairns, J. A.; Baghin, J. E. E.; Clark, G. J.; Ziegler, J. F. *J. Catal.* **1983**, *83*, 301. Sadeghi, H. R.; Henrich, V. E. *J. Catal.* **1984**, *87*, 279.

(4) Sinfelt, J. H.; Via, G. H.; Lytle, F. W. *J. Chem. Phys.* **1977**, *67*, 3831.

(5) van Zon, J. B. A. D.; Koningsberger, D. C.; van't Blik, H. F. J.; Sayers, D. E. *J. Chem. Phys.* **1985**, *12*, 5742.

(6) Koningsberger, D. C.; van Zon, J. B. A. D.; van't Blik, H. F. J.; Visser, G. J.; Prins, R.; Mansour, A. N.; Sayers, D. E.; Short, D. R.; Katzer, J. R. *J. Phys. Chem.* **1985**, *89*, 4075.

(7) Koningsberger, D. C.; van't Blik, H. F. J.; van Zon, J. B. A. D.; Prins, R. In *Proceedings of the 8th International Congress on Catalysis*; Verlag Chemie: Basel, 1984; Vol. V, p 123.

(8) Kent, S. A. Thesis, University of Delaware, 1975.

(9) Cook, J. W.; Sayers, D. E. *J. Appl. Phys.* **1981**, *52*, 5024.

(10) Martens, J. H. A.; Zandbergen, H. W.; Koningsberger, D. C.; Prins, R., to be submitted for publication.

(11) Wyckhoff, R. W. G. *Crystal Structures*; 2nd. ed.; Wiley: New York, 1963; Vol. 1, p 10.

(12) Coey, J. M. *Acta Crystallogr., Sect. B: Struct. Crystallogr. Cryst. Chem.* **1970**, *26*, 1876.

(13) *Structure Reports for 1964*; Pearson, W. B., Ed.; A. Oosthoek Uitgevers Maatschappij N.V.: Utrecht, 1972, Vol. 29, p 130.

(14) van't Blik, H. F. J.; van Zon, J. B. A. D.; Huizinga, T.; Vis, J. C.; Koningsberger, D. C.; Prins, R. *J. Am. Chem. Soc.* **1985**, *107*, 3139.

TABLE II: Structural Parameters^a Obtained from the EXAFS Analysis

| | Rh-Rh | | | Rh-O | | | Rh-Ti | | |
|--------------------------|----------|--------------|---|----------|--------------|---|----------|--------------|---|
| | <i>N</i> | <i>R</i> , Å | $\Delta\sigma^2 \times 10^3$, Å ² | <i>N</i> | <i>R</i> , Å | $\Delta\sigma^2 \times 10^3$, Å ² | <i>N</i> | <i>R</i> , Å | $\Delta\sigma^2 \times 10^3$, Å ² |
| $T_{\text{red}} = 473$ K | 3.1 | 2.67 | 5.0 | 2.5 | 2.71 | 0 | | | |
| $T_{\text{red}} = 673$ K | 3.3 | 2.63 | 3.8 | 2.1 | 2.67 | 2.2 | 2.65 | 3.42 | 4.4 |
| estd error | ±0.3 | ±0.01 | ±0.2 | ±0.5 | ±0.02 | ±1 | ±0.5 | ±0.02 | ±1 |

^a*N* = average number of neighbors. *R* = average coordination distance. $\Delta\sigma^2$ = the Debye-Waller factor relative to the reference compound.

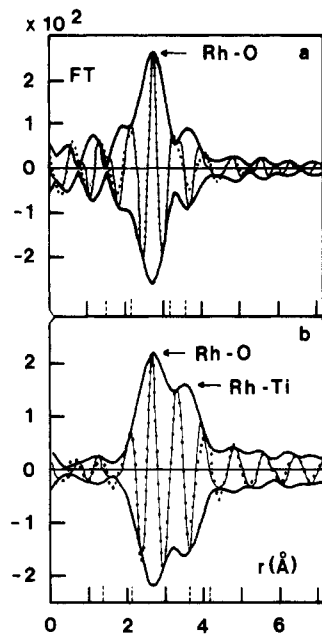


Figure 2. A comparison of the magnitudes and imaginary parts of the Fourier transforms of the difference files for the normal (a) and SMSI (b) states. The transforms are k^1 weighed, corrected for Rh-O phase, and taken over a range of 4–9 Å⁻¹. Also shown as dotted curves are the imaginary parts of the Fourier transforms of the calculated spectra for Rh-O (a) and Rh-O + Rh-Ti (b).

14. For both spectra a Rh-Rh nearest-neighbor contribution, calculated from the optimized Rh-Rh structural parameters (see Table II), was subtracted from the measured spectrum.

The resulting difference spectra were Fourier transformed (corrected for the Rh-O phase shift obtained from EXAFS measurements on Rh₂O₃⁵). The magnitude and imaginary part of the spectra are shown in Figure 2, a and b. It can be seen that the imaginary part of the Rh-O phase corrected Fourier transform of the residual spectrum obtained for the sample reduced at 473 K is symmetric and peaks at 2.71 Å, demonstrating that this peak is due to oxygen. Following the results derived in our earlier papers,⁵⁻⁷ we concluded that these oxygen neighbors arise from rhodium-oxygen bonds present in the metal-support interface. Back-transformation of the main peak in Figure 2a over a range of 1.5–3.6 Å and fitting in *k* space resulted in the structural parameters for this Rh-O coordination given in Table II. The reliability of the Rh-O coordination parameters has been checked by comparing the imaginary part of the Fourier transform of the difference spectrum with the corresponding transform of the Rh-O EXAFS function calculated with these parameters. This is also shown in Figure 2a as indicated. Within the *r* region for back-transformation to *k* space both transforms are very similar, although small differences can be detected particularly between 1.5 and 2.2 Å and between 3.2 and 3.6 Å.

The Rh-O phase corrected Fourier transform of the difference spectrum for the sample reduced at 673 K (Figure 2b) clearly shows the presence of two dominant contributions. The first peak is similar to the oxygen coordination found at 473 K. The most probable origin of the second peak is a Ti neighbor as is discussed below. Since oxygen may also be a scatterer, this possibility was included in further analysis. The phase shift and backscattering amplitude functions for the Rh-Ti absorber scatterer pair were obtained from EXAFS measurements on a RhTi alloy.¹⁰ Again

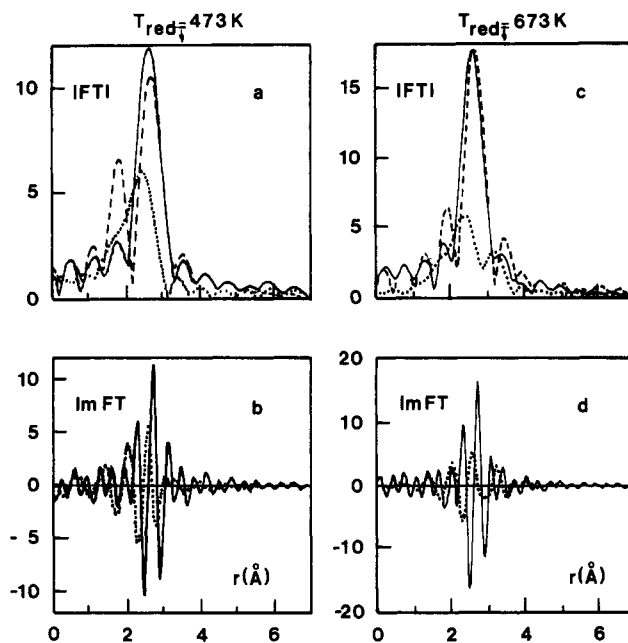


Figure 3. (a,c) Comparison between the magnitude of the Fourier transforms of the experimental data (dashed curve) and the separate Rh-Rh (solid curve) and Rh-O (a) or Rh-O + Rh-Ti (c) contributions (dotted lines) for the normal and the SMSI states, respectively. (b, d) Comparison between the imaginary parts of the Fourier transforms of the separate Rh-Rh (solid curve) and Rh-O (b) or Rh-O + Rh-Ti (d) contributions (dotted lines) for both states. The Fourier transforms are k^3 weighed, corrected for the Rh-Rh phase and amplitude, and taken from 4 to 10 Å⁻¹.

the main peak in Figure 2b was back-transformed to *k* space with a range of 1.4–4.2 Å. The best two-shell fit in *k* space was obtained using one Rh-O and one Rh-Ti contribution. The structural parameters which led to the best agreement between the calculated Rh-O + Rh-Ti EXAFS function and the difference spectrum both in *k* space and in *r* space between their corresponding Fourier transforms are summarized in Table II. Figure 2b shows that the imaginary parts of both transforms are very similar. Within the region for back-transformation again, small differences in the regions of 1.4–2.2 Å and 3.6–4.2 Å can be seen.

The amplitude of the calculated Rh-O and Rh-O + Rh-Ti EXAFS functions can be best compared with those of the calculated Rh-Rh and the experimental EXAFS data by transforming all functions under identical conditions. The magnitudes and imaginary parts of these transforms are displayed in Figure 3, a,c and b,d, respectively. The imaginary parts show clearly that by adding the different contributions interferences are created which give peaks in the magnitude of the resulting transform (dashed curve) at positions different from those of the individual components.

The agreement between the calculated Rh-Rh + Rh-O ($T_{\text{red}} = 473$ K) and Rh-Rh + Rh-O + Rh-Ti ($T_{\text{red}} = 673$ K) EXAFS functions and the corresponding experimental data can be seen in Figure 1, c and f, where the imaginary parts of the two corresponding EXAFS functions are plotted for both reduction temperatures. It can be seen that almost all features of the experimental data are reproduced by the calculated EXAFS functions. Still detectable but small differences can be noticed which correspond to those found for the difference files (see Figure 2a,b).

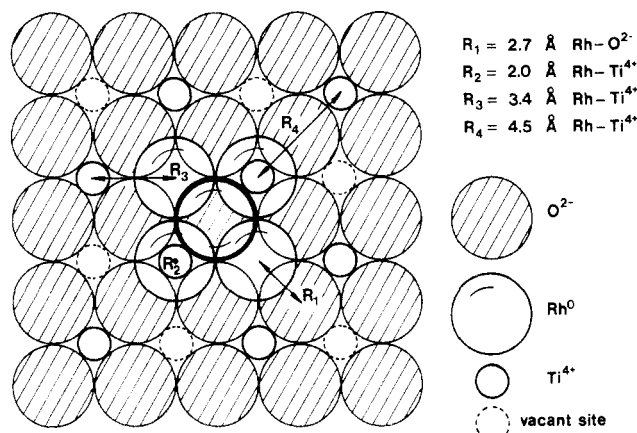


Figure 4. Model of rhodium five-atom particle resting on an anatase [001] surface.

Discussion

Although the measurements were performed under H₂ atmosphere, the Rh-Rh coordination distance as well as the disorder diminished markedly (viz. 2.63 vs. 2.67 Å, 3.8×10^{-3} vs. 5×10^{-3} Å²) after reduction at 673 K. Lowering of the average coordination distance for a Rh/Al₂O₃ catalyst (measured after reduction and evacuation) has been ascribed to contraction of the metal particle, due to desorption of H₂.¹⁵ Obviously, the metal particles in the Rh/TiO₂ catalyst reduced at 673 K are not covered with chemisorbed hydrogen. The coordination number of the 2.7-Å Rh-O bond did not increase after reduction at 673 K, which demonstrates that coverage of the metal particles had not taken place. In addition to Rh-Rh and Rh-O contributions, observed for both samples, after reduction at 673 K a Rh-Ti coordination at 3.42 Å has been found. The Rh-Ti distance at 2.676 Å as in the RhTi alloy has not been found for either state of the catalyst. This indicates that alloy formation had not taken place. The major difference between the 473 and 673 K reduced sample is the pronounced presence of a Rh-Tiⁿ⁺ coordination at about 3.4 Å. We feel that the understanding of the origin of the SMSI state has to be found in this Rh-Ti coordination.

At normal temperatures, the majority of the surface of anatase consists of [001] layers of oxygen ions in which half of the octahedral sites are occupied by Ti⁴⁺ ions.¹⁶ The following structural model can now be derived based upon the coordination parameters given in Table II. The average Rh-Rh coordination number of 3.2 and the Rh-O coordination number of 2.4 correspond to particles of five metal atoms, four of which are in contact with the support (see Figure 4). It has been discussed in ref 5 that the use of the Rh³⁺-O²⁻ absorber scatterer pair as reference compound for the determination of the Rh⁰-O²⁻ support coordination

number leads to values which will be 0-30% too low. Each of the four interfacial metal atoms might then have four oxygen nearest neighbors at 2.7 Å (R_1 in Figure 4); two of them have one Ti⁴⁺ at 2.0 Å (R_2 in Figure 4) in their nearest-neighbor shell, and the other two each have four Ti⁴⁺ ions at 3.4 Å (R_3 in Figure 4). The coordination numbers of these Rh-Ti contributions averaged over all five atoms present in the particle are low ($R_2 = 2.0 \text{ \AA}$, $N_2 = 0.4$; $R_3 = 3.4 \text{ \AA}$, $N_3 = 1.6$). Due to the low coordination numbers and the low backscattering amplitude of Ti⁴⁺, their contributions to the EXAFS spectrum will be small. However, in the Fourier transform presented in Figure 2a, small differences between calculated and difference spectrum are still visible in the regions 1.5-2.2 Å and 3.2-3.6 Å possibly due to Rh-Ti distances at 2.0 and 3.4 Å, respectively.

When at high temperatures in H₂ atmosphere the TiO₂ surface starts to reduce, oxygen atoms from the first [001] layer will be removed. The second oxygen layer and bare Tiⁿ⁺ ions of the first layer will become exposed. These bare Tiⁿ⁺ ions will migrate to the vacant octahedral sites (dotted circles in Figure 4) in the second and possibly third oxygen layer. As a consequence, the second and third oxygen layers will resemble a shear plane as in Ti₄O₇. The metal atoms in the metal-support interface which now rest on this second oxygen layer will experience the enhanced presence of Tiⁿ⁺ ions. Indeed, for the 673 K reduced sample a strongly enhanced 3.4-Å Rh-Tiⁿ⁺ contribution has been observed. In Figure 2b (the Fourier transform of the best simulation for the 673 K reduced sample) differences in the region 1.4-2.2 Å (due to a distance at 2.0 Å) and even in the region 3.6-4.7 Å (due to a distance at 4.5 Å, R_4 in Figure 4) remain visible.

On the basis of these results, we propose that the structure of a small TiO₂ supported Rh particle in the SMSI state is as follows. The metal particles rest on an [001] layer of reduced TiO₂, a layer that closely resembles a shear plane in Ti₄O₇. Surprisingly, in these results there is no evidence for coverage of the metal particle with a suboxide of TiO₂, the model that has been generally accepted during the past years as the origin for the anomalous properties of the metal particle.³ Since we found no evidence for alloy formation as well, we feel that the special, probably electronic properties of this suboxide are responsible for the SMSI state. To clarify this, however, more research will have to be done. The results of such research and of a more detailed analysis of the spectra discussed here will be the subject in a more extensive publication.

Acknowledgment. This work was done at SSRL (Stanford University), which is supported by the Department of Energy, The National Science Foundation, and the National Institutes of Health. We gratefully acknowledge the assistance of the SSRL staff and the assistance of Dr. Gajardo and Dr. Michel in the preparation and characterization of the catalyst. This study was supported by the Netherlands Foundation for Chemical Research (SON) with financial aid from the Netherlands Organization for the Advancement of Pure Research (ZWO). D.C.K. thanks ZWO for supplying a travel grant (R71-34).

Registry No. Rh, 7440-16-6; TiO₂, 13463-67-7; H₂, 1333-74-0.

(15) van't Blik, H. F. J.; van Zon, J. B. A. D.; Koningsberger, D. C.; Prins, R. *J. Mol. Catal.* **1984**, *25*, 379.

(16) Woning, J.; van Santen, R. A. *Chem. Phys. Lett.* **1983**, *101*, 541.